scientific reports

Check for updates

OPEN

Atmospheric formaldehyde production on early Mars leading to a potential formation of bio-important molecules

Shungo Koyama[1]✉, Arihiro Kamada[1], Yoshihiro Furukawa[1], Naoki Terada[1], Yuki Nakamura[2], Tatsuya Yoshida[1], Takeshi Kuroda[1,3] & Ann Carine Vandaele[4]

Formaldehyde (H_2CO) is a critical precursor for the abiotic formation of biomolecules, including amino acids and sugars, which are the building blocks of proteins and RNA. Geomorphological and geochemical evidence on Mars indicates a temperate environment compatible with the existence of surface liquid water during its early history at 3.8–3.6 billion years ago (Ga), which was maintained by the warming effect of reducing gases, such as H_2. However, it remains uncertain whether such a temperate and weakly reducing surface environment on early Mars was suitable for producing H_2CO. In this study, we investigated the atmospheric production of H_2CO on early Mars using a 1-D photochemical model assuming a thick CO_2-dominated atmosphere with H_2 and CO. Our results show that a continuous supply of atmospheric H_2CO can be used to form various organic compounds, including amino acids and sugars. This could be a possible origin for the organic matter observed on the Martian surface. Given the previously reported conversion rate from H_2CO into ribose, the calculated H_2CO deposition flux suggests a continuous supply of bio-important sugars on early Mars, particularly during the Noachian and early Hesperian periods.

Present-day Mars is extremely cold and dry, but many geomorphological and geochemical evidence, such as valley networks, suggest an active water cycle at 3.8–3.6 Ga[1]. The detection of phyllosilicates over the Noachian terrain also supports the existence of widespread liquid water on early Mars[2]. The habitability of Mars has been of great interest that triggered previous and ongoing Martian explorations. Although water is a probable requirement of Martian habitability, this molecule is not an organic compound in genomic and catalytic bio-molecules that supports the fundamentals of life. Investigations on the organic synthesis on ancient Mars fill the gap by verifying the possibility, environment, and age of the chemical evolution to potential ancient Martian life.

Formaldehyde (H_2CO) is simple organic matter that can be formed through various chemical reactions in planetary atmospheres. H_2CO is a highly soluble and reactive molecule, and thus has the potential to play a significant role in the abiotic formation of bioorganic molecules[3]. For example, amino acids are formed by reactions involving H_2CO, NH_3, and HCN via the Strecker reaction[4]. Additionally, in ammonia-involving formose-type reactions, the condensation of H_2CO with NH_3 yields various amino acids[5,6]. The formose reaction is a thermally driven aqueous process that generates many sugars from H_2CO, including ribose, a fundamental building block of RNA that is regarded as a key molecule for the origin of life[7–9]. Therefore, determining whether the surface environments on early terrestrial planets fostered the production of H_2CO is crucial for understanding prebiotic chemical evolution to the origin of life.

The evidence that supports the existence of liquid water have led many scientists to imagine a warm early Martian climate as it is on Earth[1,2]. Previous numerical studies have attempted to reproduce warm early Mars; however, 3-D global circulation model (GCM) studies have not been able to reproduce the continuous presence of liquid water on the surface with CO_2-H_2O atmospheres[10,11]. To reconcile this geomorphological evidence, episodic melting scenarios driven by the supply of reducing gases through volcanic outgassing or meteorite impacts have been proposed[12–15].

[1]Graduate School of Science, Tohoku University, Sendai, Miyagi 980-8578, Japan. [2]Graduate School of Science, The University of Tokyo, Tokyo, Japan. [3]Division for the Establishment of Frontier Sciences of Organization for Advanced Studies, Tohoku University, Sendai, Japan. [4]Royal Belgian Institute for Space Aeronomy, BIRA-IASB, Brussels, Belgium. ✉email: koyama.shungo.q5@dc.tohoku.ac.jp

Pinto et al.[16] provided an estimate for the photochemical production of H_2CO in the N_2-dominated atmosphere of primitive Earth, with the number density of H_2CO near the surface approximated to be ~ 10^8 cm^{-3}. A similar amount of H_2CO production was also predicted for early Earth conditions by Harman et al.[17]. However, the production of H_2CO in a CO_2-dominated atmosphere on early Mars has not yet been thoroughly investigated. Understanding its production on early Mars can provide insights into the potential of life on the planet.

In this study, we investigated the production of H_2CO in a thick CO_2-dominated atmosphere containing H_2 and CO on early Mars using a 1-D photochemical model. We then estimated ribose production using our simulation results and experimental data.

Methods

Model description

To calculate the atmospheric production of H_2CO, we adapt a one-dimensional photochemical model, PROTEUS (Photochemical and RaiatiOn Transport model for Extensive USe), detailed by Nakamura et al.[18], for early Martian conditions. This model has been successfully applied to other planetary atmospheres, such as the Jovian ionosphere[19] and present-day Martian atmosphere[20]. It solves the continuity equations involving chemical reactions and vertical transport until the profiles of each species reach a steady state. We consider 63 chemical reactions (Supplementary Table S1 online) for 8 neutrals: CO_2, CO, H_2, H_2O, O_2, H_2O_2, O_3, H_2CO, 6 radicals: H, O, OH, HO_2, $O(^1D)$, HCO, and an ion of CO_2^+ in a 2-bar CO_2-dominated atmosphere. Though the atmospheric surface pressure of early Mars is still not well constrained, 3-D global circulation model studies suggest that a 2 bar CO_2 atmosphere with a few percentages of reducing gas is required for a warm climate[14,15]. The exobase altitude is defined as a pressure level of 10^{-9} mbar. We utilize the H_2O vapor number density and temperature profiles up to ~ 60 km (Fig. 1) from the 2-bar global mean results with an obliquity of 40° computed using a 3-D paleo-Mars global climate model[15,21]. The global climate model assumed three scenarios of an atmosphere containing 0, 3, and 6% H_2. For the H_2O density profiles above ~ 60 km, we assume the same mixing ratio up to the exobase, assuming the effect of cold trap. The sensitivity to the H_2O vapor content in the atmosphere is discussed in Results section. For temperature, we assume isothermal up to the lower boundary of the thermosphere (6×10^{-3} Pa) considering radiative equilibrium and then extrapolate it into the thermosphere[22,23]. The exobase temperature is fixed at 800 K, corresponding to 10 × EUV at 3.8 Ga[24]. We adopt the solar spectrum from 3.8 Ga estimated by Claire et al.[25]. We use the updated H_2O absorption cross section measured by Ranjan et al[26]. We assume the up-to-date absorption cross sections for all the species to the best of our knowledge. References for cross sections of all species at each wavelength are presented in Nakamura et al.[18]. The CO_2^+ concentration profile calculated by the ionosphere photochemistry model[27] is fixed at the same pressure altitude as present-day Mars to represent the dissociation reaction of H_2 with CO_2^+ to produce atomic H in the upper atmosphere, allowing

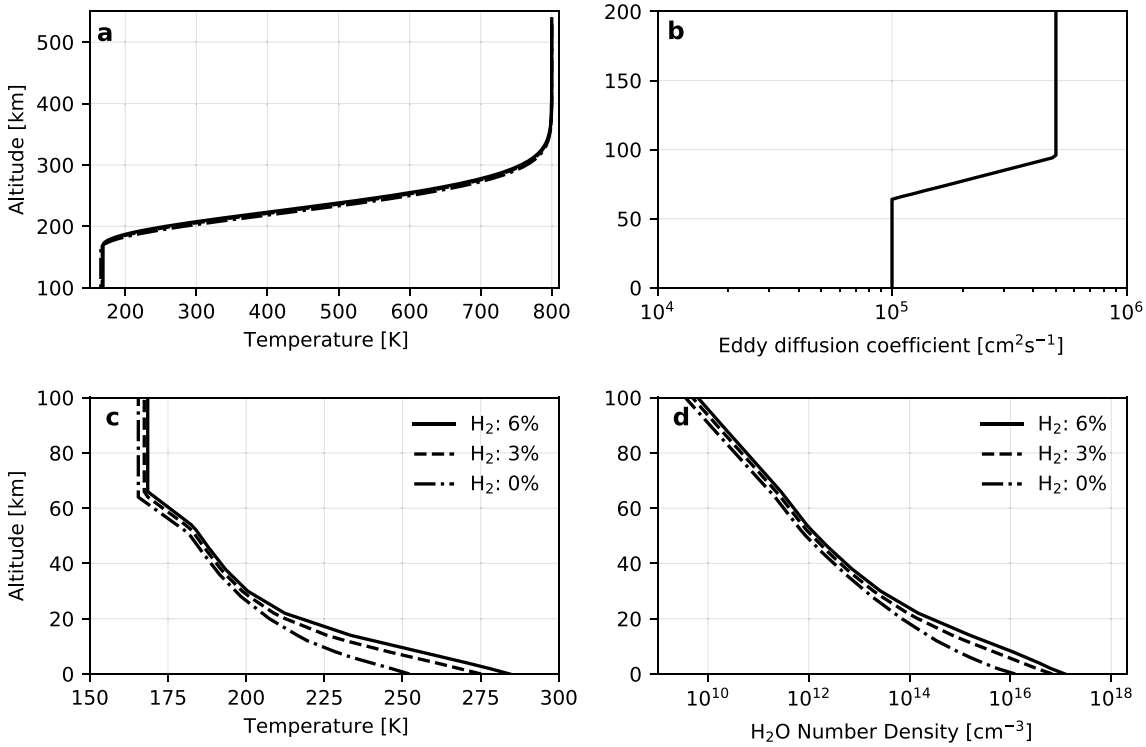

Figure 1. Background atmospheric conditions in early Mars. Temperature-altitude profile (**a** and **c**), Eddy diffusion coefficient profile (**b**), and H_2O number density profile (**d**). The solid, dashed, and dash-dotted lines correspond to H_2 6%, 3%, and 0% conditions, respectively. The temperature and H_2O number density profiles of the H_2 0% case in this figure are used to calculate the results for H2 0.1, 0.01, 0.001, and 0.0001% cases.

us to calculate the escape flux of hydrogen[23]. Although the density of CO_2^+ in the early Martian atmosphere has uncertainty, its profile has little impact on the result, because the escape flux of hydrogen is limited by H_2 diffusion from the lower atmosphere. We adopt eddy diffusion coefficient profiles using the typical formula adapted for other planets than Earth[28]. The vertical temperature, H_2O number density, and eddy diffusion coefficient profiles are shown in Fig. 1. The temperature and water vapor profiles of the H_2 0% scenario shown in Fig. 1 are used to calculate the H_2CO production under the conditions of 0.1, 0.01, 0.001, and 0.0001% H_2.

For the upper boundary, we assume Jeans escape of H and H_2 and fix the O escape rate at 2.6×10^8 cm^{-2} s^{-1} corresponding to 10 × EUV conditions[24]. The O escape rate does not have a large impact on the results because it does not control O_2 abundance in the lower atmosphere where H_2CO is dominantly produced. Deposition velocities are applied to H_2O_2, HO_2, H_2CO, HCO, OH, O, and H[29,30]. The deposition velocities of each species are shown in Supplementary Table S2 online. We compute the dry deposition of H_2CO by imposing the deposition velocity. This model also includes the rainout of H_2CO throughout the atmosphere using the same parameterization as Hu et al[28]:

$$k_R(z) = f_R \times \frac{n_{H_2O}(z)k_{H_2O}(z)}{55N_A\left[L \times 10^{-9} + \left(H'RT(z)\right)^{-1}\right]}, \quad (1)$$

where k_R is rainout frequency, f_R is a reduction factor which is an adjustable parameter to represent the reduction relative to Earth's hydrological cycle, n_{H_2O} is the number density of H_2O, k_{H_2O} is the precipitation rate assumed to be 2×10^{-6} s^{-1}, N_A is Avogadro's constant, L is the liquid water content assumed to be 1 g m^{-3}, H′ is the effective Henry's Law constant assumed to be 1.3×10^4 M atm^{-1} taken from Giorgi & Chameides[31], R is gas constant, and T is temperature. The rainout rate is then obtained by multiplying k_R by number density of H_2CO. We assume f_R to be 1, assuming that early Mars had a hydrological cycle similar to Earth's. Sensitivity to f_R is discussed in Results section. The boundary conditions for H_2 and CO are fixed in the calculation of H_2CO production in the results. We impose H_2 outgassing and CO deposition velocity as a boundary condition to determine the possible range of H_2 and CO mixing ratio in the following section.

Background H_2 and CO atmospheric conditions

Potential sources of H_2 gas on early Mars include volcanic degassing[29], meteorite impacts[32–34], and serpentinization[35]. The upper limit of the H_2 outgassing rate is estimated to be 8×10^{11} cm^{-2} s^{-1} considering the supplies from volcanism and serpentinization[29]. We computed H_2 mixing ratios in a background 2-bar CO_2 atmosphere for various H_2 outgassing rates to investigate the plausibility of CO_2 atmospheres enriched in H_2, assuming a fixed CO deposition velocity of 10^{-8} cm s^{-1}[29] (see Supplementary Fig. S1 online). An H_2 outgassing rate of ~ 5×10^{11} cm^{-2} s^{-1} yields a 5–6% H_2 mixing ratio in a 2-bar CO_2 atmosphere. This result is consistent with that of Batalha et al.[29], in which an H_2 outgassing rate of 8×10^{11} cm^{-2} s^{-1} yields a ~ 5% H_2 mixing ratio in a 3-bar CO_2 atmosphere. The minimum value of the H_2 mixing ratio is ~ 1×10^{-6} when assuming the absence of H_2 degassing. Furthermore, Chassefiere et al.[35] suggested that serpentinization-derived CH_4 trapped in the cryosphere could have been released into the atmosphere, producing a transient 1–2 bar CO_2 atmosphere containing 10–20% H_2 gas. Thus, a 6% H_2 mixing ratio in a background 2-bar CO_2 atmosphere is plausible. This study considers a range of H_2 mixing ratios from 1×10^{-6} to 0.06.

The abundance of CO on early Mars is not well constrained. A dense and cold CO_2 atmosphere is likely to enter the CO runaway state[23]. The CO and O liberated from CO_2 photolysis no longer recombine because of the lack of odd hydrogen species that catalyze CO_2 recombination. Moreover, because the equilibrium timescale of CO is relatively long, ranging from several million to several hundred million years[23], it is insufficient to consider only a single steady state condition. Therefore, it is necessary to vary the CO mixing ratio as a parameter within a specific range.

To determine the possible CO range, we calculated the CO mixing ratios over a wide range of CO deposition velocities for 0, 3, and 6% H_2 cases. Different temperatures and H_2O profiles are used for each H_2 case obtained from the GCM results[15]. We assume a free lower boundary condition for H_2 in the 0% H_2 case, whereas the number density is fixed for the 3 and 6% H_2 conditions.

As a result, the 0% H_2 case enters a CO runaway state with a low CO deposition velocity of $< 10^{-10}$ cm s^{-1} (see Supplementary Fig. S2 online) as suggested by the previous photochemical model study of early Mars conditions[36]. Conversely, warmer atmospheres containing 3 or 6% H_2 have a maximum CO mixing ratio of ~ 1% because sufficient H_2O vapor promotes CO_2 recombination. The CO deposition velocity on an abiotic ocean planet is estimated to be 10^{-9}–10^{-8} cm s^{-1}[37,38]; however, there is no known efficient process to remove CO at the surface without the ocean[28]. Considering that ancient Mars experienced episodic cold and warm climates[1], a CO_2 atmosphere would have been in a CO runaway state during the ice age[36], while the atmosphere would have been stable with a minimum CO mixing ratio of 1% in warmer climates. Based on these results, the possible range of CO on early Mars should be from 1 to 50%.

Results

Photochemical production of formaldehyde

The present 1-D photochemical model shows that H_2CO forms at number densities of ~ 5×10^9 and ~ 7×10^{-2} cm^{-3} near the surface under 6% H_2 condition and 0.01% H_2 condition, respectively (Fig. 2). Production in a 6% H_2 atmosphere is substantial; approximately 50 times higher than that estimated for Earth's Hadean atmosphere[16].

H_2CO is predominantly formed through a radical–radical reaction of two HCO molecules[39]:

$$HCO + HCO \rightarrow H_2CO + CO. \quad (R1)$$

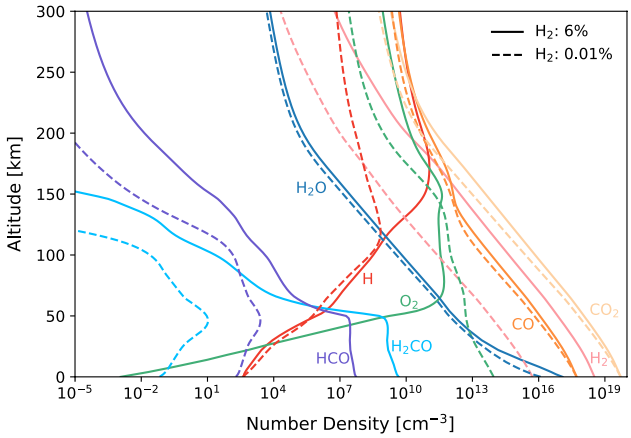

Figure 2. Number density profiles of main species under the 6% H_2 (solid line) and 0.01% H_2 (dashed line) conditions. CO is fixed at 1% in both cases.

The dominant production path of HCO is a three-body reaction of H and CO:

$$H + CO + M \rightarrow HCO + M, \tag{R2}$$

where M represents the background gas, mainly CO_2 in this model. In the early Martian atmosphere, H and CO in R2 are derived from H_2O and CO_2 photolysis, respectively. HCO is dominantly destroyed by a reaction with O_2:

$$HCO + O_2 \rightarrow HO_2 + CO. \tag{R3}$$

These reactions imply that the production of H_2CO decreases with O_2 because O_2 reacts with HCO through R3, thereby reducing the rate of R1.

The H_2CO production in the 6% H_2 atmosphere is notably higher than that under lower H_2 conditions. This results from the discrepancy in the O_2 abundance in the lower atmosphere between these two conditions. There is a sharp decline in the O_2 density below 60 km for 6% H_2 (Fig. 2). The lack of O_2 in the 6% H_2 atmosphere decreased the reaction rate of HCO with O_2 (R3). Consequently, a larger amount of HCO remains near the surface, ultimately increasing the amount of H_2CO via reaction R1. Two mechanisms below contribute to the decrease in O_2.

The first mechanism is driven by H atoms at altitudes greater than 100 km. The source of O_2 near the surface is the downward transport of O_2 liberated from CO_2 photolysis at high altitudes. The significant difference between the 6% and 0.01% H_2 cases is the number of H atoms at altitudes above 100 km. H_2 is transported upward and photolyzed into H atoms by the solar UV flux, producing more H in the 6% H_2 case. O_2 reacts with H at high altitudes and is converted back into CO_2 via the following reaction:

$$H + O_2 + M \rightarrow HO_2 + M \tag{R4}$$

$$H + HO_2 \rightarrow 2OH \tag{R5}$$

$$CO + OH \rightarrow CO_2 + H. \tag{R6}$$

The altitude profiles of the reaction rate of R4 between the 6% and 0.01% H_2 cases indicate that R4 shifted upward under the 6% H_2 condition (Fig. 3). The loss of O_2 by H atoms through R4 above ~ 150 km results in a decrease in O_2 downward flux below ~ 135 km, as shown in Fig. 4.

The second mechanism is driven by the HCO catalytic cycle. In the present-day Martian atmosphere, odd hydrogen species act as catalysts to recombine CO and O into CO_2 through the following cycle[40]:

$$H + O_2 + M \rightarrow HO_2 + M \tag{R4}$$

$$O + HO_2 \rightarrow OH + O_2 \tag{R7}$$

$$CO + OH \rightarrow CO_2 + H \tag{R6}$$

Net: $CO + O \rightarrow CO_2$.

The net result is the recombination of CO_2.

In a dense CO_2 atmosphere, HCO catalytic reactions are responsible for converting H to HO_2 in addition to R4:

$$HCO + O_2 \rightarrow HO_2 + CO \tag{R3}$$

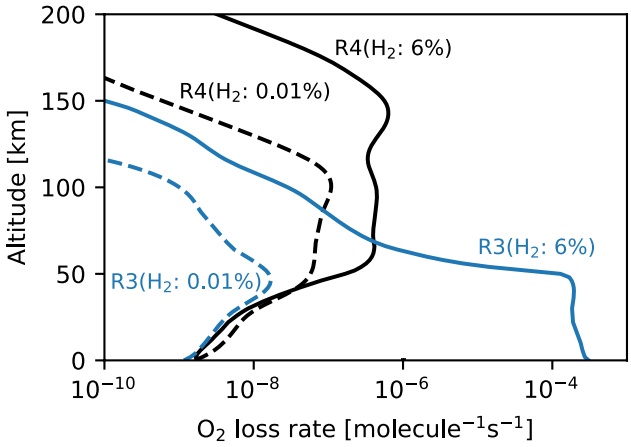

Figure 3. A comparison of O_2 loss reaction rates per one O_2 molecule (= reaction rate / O_2 number density) under the 6% H_2 (solid line) and 0.01% H_2 (dashed line) conditions. The black and blue lines show the reaction rates of $H + O_2 + M \rightarrow HO_2 + M$ (R4) and $HCO + O_2 \rightarrow HO_2 + CO$ (R3), respectively.

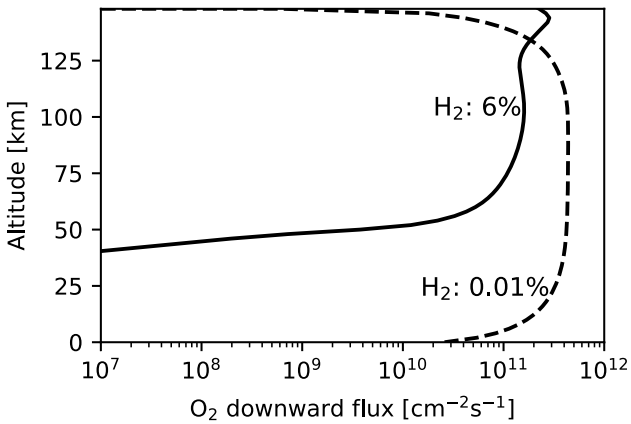

Figure 4. A comparison of O_2 downward flux profiles under the 6% H_2 (solid line) and 0.01% H_2 (dashed line) conditions.

$$H + CO + M \rightarrow HCO + M \quad \text{(R2)}$$

Net: $H + O_2 \rightarrow HO_2$.

This is because a larger amount of CO is formed in a denser atmosphere owing to the lack of amounts of odd hydrogen, while O_2 is more abundant than CO in the present-day Martian atmosphere. The reaction rate profile of R3 in a 6% H_2 atmosphere indicates that the HCO catalytic cycle dominates at ~ 50–60 km (Fig. 3), where the O_2 density declines sharply (Fig. 2). This cycle significantly reduces O_2 in the lower atmosphere below 50–60 km.

Deposition of formaldehyde

A 6% H_2 mixing ratio enables the presence of an ocean in a warm climate[15]. In a warm environment with an ocean and a CO deposition velocity of 10^{-8}–10^{-9} cm s^{-1}[37,38], the CO mixing ratio is ~ 1%, as shown in the 3% and 6% H_2 cases in Supplementary Fig. S2. Consequently, the deposition flux of H_2CO into the surface liquid water is approximately 3×10^9 cm^{-2} s^{-1} in a warm climate.

When the mixing ratio of H_2 and CO decreases, the deposition of H_2CO decreases. However, the H_2CO decrease is not gradual, and there is a respective large drop with the decrease in H_2 and CO. Large amounts of H_2CO are deposited in an atmosphere containing either > 0.1% H_2 or > 50% CO (Fig. 5).

The high-altitude H generates a large drop between 0.01 and 0.1% H_2, as shown in Fig. 5. The large decrease between 10 and 50% CO is associated with the HCO catalytic cycle (Fig. 5). Increasing the CO produces more HCO (R2), thereby removing O_2 in the lower atmosphere (R3). In an atmosphere containing 10% CO, a steady state is reached with more O_2 and less HCO. Conversely, the atmosphere containing 50% CO reaches a steady state with less O_2 and more HCO. Therefore, in an atmosphere with H_2 < 0.01%, more H_2CO is produced with 50% CO.

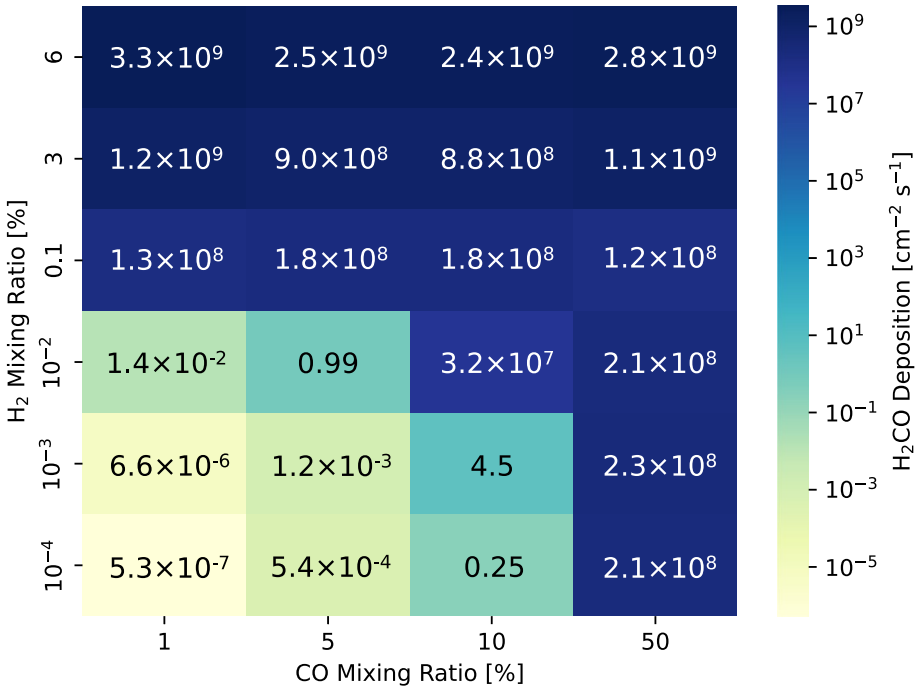

Figure 5. H_2CO deposition flux as a function of CO and H_2 mixing ratios assuming a 2-bar CO_2 background atmosphere.

Formaldehyde deposition in more abundant H_2 and H_2O conditions

We first assessed the impact of a higher H_2 mixing ratio than 6% on H_2CO production, with the CO mixing ratio fixed at 1% and H_2O and temperature profiles from the 6% H_2 GCM results[15]. This assumption may not represent early Martian conditions, but it allows the estimation of the upper limit of H_2CO production in a CO_2-dominated atmosphere on early Mars and provides insights into an exoplanet analog for a CO_2-dominated atmosphere enriched with H_2. As shown in Fig. 6, increasing the H_2 mixing ratio from 1 to 20% increased the H_2CO deposition slightly. However, the deposition flux does not exceed 5×10^9 cm^{-2} s^{-1}. This result implies that H_2CO production under early Martian atmospheric conditions would be close to its maximum in H_2-rich CO_2-dominated atmospheres.

Subsequently, we multiplied the H_2O profile of the 6% H_2 case by a factor ranging from 0.01 to 100 while maintaining the H_2 and CO mixing ratios at 6% and 1%, respectively, with the temperature profile of the 6% H_2 case. This approach accounts for spatiotemporal variations in water vapor content on a global scale. H_2O vapor changes by ~ 10 times over the global scale in the global climate model results[21]. Considering the seasonal difference, changes by ~ 2 orders of magnitude are reasonable for early Mars conditions. As an upper and lower limit, we changed the amount of H_2O vapor by 4 orders of magnitude. This parameter survey may also be useful for exoplanets' environment. A higher water vapor content significantly increases H_2CO production (Fig. 6b). The H_2CO deposition flux increases up to ~ 1×10^{12} cm^{-2} s^{-1} with a 100 times higher H_2O density. Under conditions of abundant H_2O, additional H atoms are generated through H_2O photolysis, resulting in increased HCO formation through R2 and, consequently, greater H_2CO production through R1. In addition, an increase in precipitation also contributes to the increased rainout rate of H_2CO. This indicates that in a warm climate with 6% H_2, the limiting factor for H_2CO production is not H_2 but the abundance of H_2O. The timescale for the change in H_2CO formation due to variations in water vapor content is a few years in our calculation. This result suggests that H_2CO production on early Mars exhibited local variations depending on the availability of water vapor. However, further studies are needed to clarify this effect, as horizontal transport may mitigate differences in H_2CO abundance.

We also investigated the effect of the reduction factor f_R in Eq. (1) on H_2CO deposition flux. The calculated H_2CO deposition fluxes with a reduction factor of 0.1, 0.5, and 1 are shown in Supplementary Fig. S4. In this calculation, H_2 and CO mixing ratios are fixed at 6% and 1%, respectively, with temperature and H_2O profiles of the 6% H_2 case. When f_R is set to 0.1, it is reduced to 8×10^8 cm^{-2} s^{-1}, approximately 1/4 of the value when f_R is 1. Although it is not yet constrained, GCM results suggest that globally averaged precipitation on early Mars may have been 10 times smaller than on Earth[15]. Further modeling studies combining photochemistry with GCM would be helpful for a more accurate estimation of the rainout rate.

Discussion

Formation of formaldehyde throughout Mars' history

The deposition rate of H_2CO reaches the order of 10^8 or 10^9 cm^{-2} s^{-1} under conditions where the mixing ratio of H_2 is higher than 0.1%, regardless of the CO mixing ratio (Fig. 5). The H_2 mixing ratio of 0.1% is equivalent to ~ 10^{10} cm^{-2} s^{-1} of H_2 outgassing rate in a steady state (Supplementary Fig. S1). This rate is comparable to the

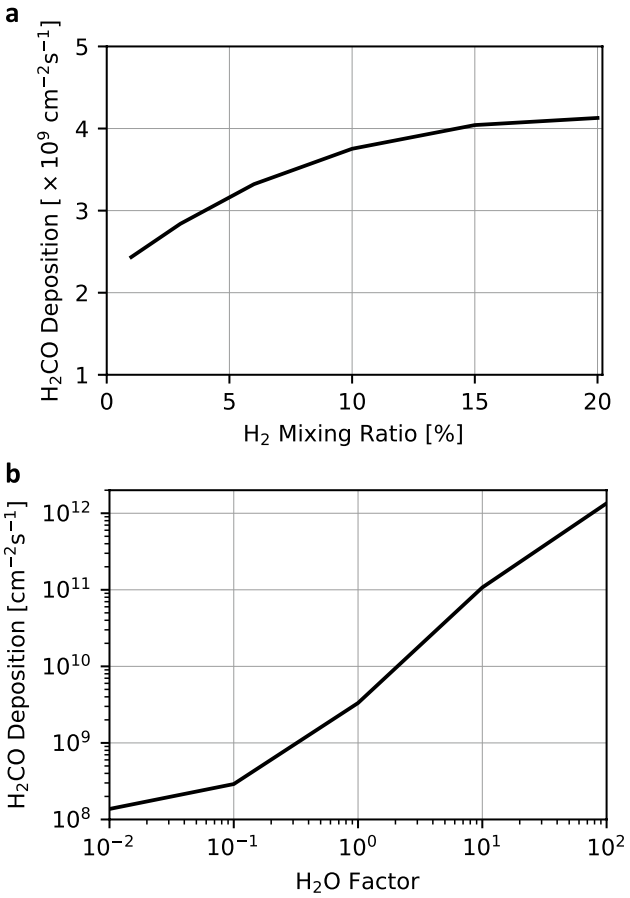

Figure 6. H_2CO deposition fluxes as a function of the H_2 mixing ratio (**a**) and H_2O factor (**b**). The temperature profile of the 6% H_2 case is used for both calculations. The bottom panel (**b**) shows H_2CO deposition fluxes obtained by multiplying the H_2O profile of the 6% H_2 case by a factor ranging from 0.01 to 100.

estimated H_2 degassing rates on present-day Earth, which has an upper mantle of quartz-fayalite-magnetite (QFM) oxidation buffer[29,41]. The H_2 degassing rate on early Mars is unclear. However, Martian meteorites suggest that the mantle was more reduced than the Earth's upper mantle, with oxygen fugacity around the iron-wüstite (IW) buffer[42,43]. Given that the oxygen fugacity of the Martian upper mantle was buffered near IW + 1, the H_2 degassing rate is estimated to be ~ 10^{11} cm^{-2} s^{-1}[29,41]. This suggests that the large atmospheric production of H_2CO continued during past periods of active volcanic degassing, regardless of the CO mixing ratio (Fig. 7). An increase in the H_2 mixing ratio from 0.1 to 6% increases the H_2CO deposition rate by approximately 10 times the global mean value (Fig. 5). This increase was mainly due to the increase in the number density of H_2O by 10 times due to the warming effect of increasing H_2 (Fig. 1d). The number density of H_2O in the atmosphere also differs (e.g., 10 times) depending on the local availability of H_2O[15]. This difference could provide local H_2CO deposition rates on Mars that are several tens of times higher and lower than the global mean value (Fig. 6b).

Volcanic degassing would have decreased from the late Hesperian to the Amazonian, decreasing the mixing ratio of H_2 and H_2O in the atmosphere[42]. A decrease in the H_2 mixing ratio to below 0.1% dramatically decreased the H_2CO deposition rate by a factor of 10^{-10} (Fig. 5). Thus, the late Hesperian to early Amazonian was a transitional period from a high to a meager H_2CO deposition rate (Fig. 7).

Formation of organic compounds in the ocean

The continuous conversion of CO_2 and CO into highly soluble H_2CO in the early Martian atmosphere may have transferred carbon from the atmosphere to the ocean. Another mechanism that converts atmospheric carbon into H_2CO involves iron-rich asteroids/meteorites[44]. Such impacts might have formed H_2CO, both locally and temporally. The overall impact-induced production would have been smaller than the continuous global production of H_2CO in the atmosphere through the photochemical reactions presented in this study (see Supplementary text online). Another source of H_2CO discussed previously is the oxidation of CH_4 with iron oxide, which was proposed to explain the tentative detection of H_2CO on present-day Mars[45].

H_2CO is highly reactive. Carbon transferred from the atmosphere as H_2CO could further be converted into various organic compounds. One of the most well-known reactions is the formose reaction, in which formaldehyde oligomerizes to form various sugar molecules in alkaline solutions[7]. A recent study found that this type of reaction can form sugars, including ribose, even in neutral solutions[46]. To estimate ribose production in the

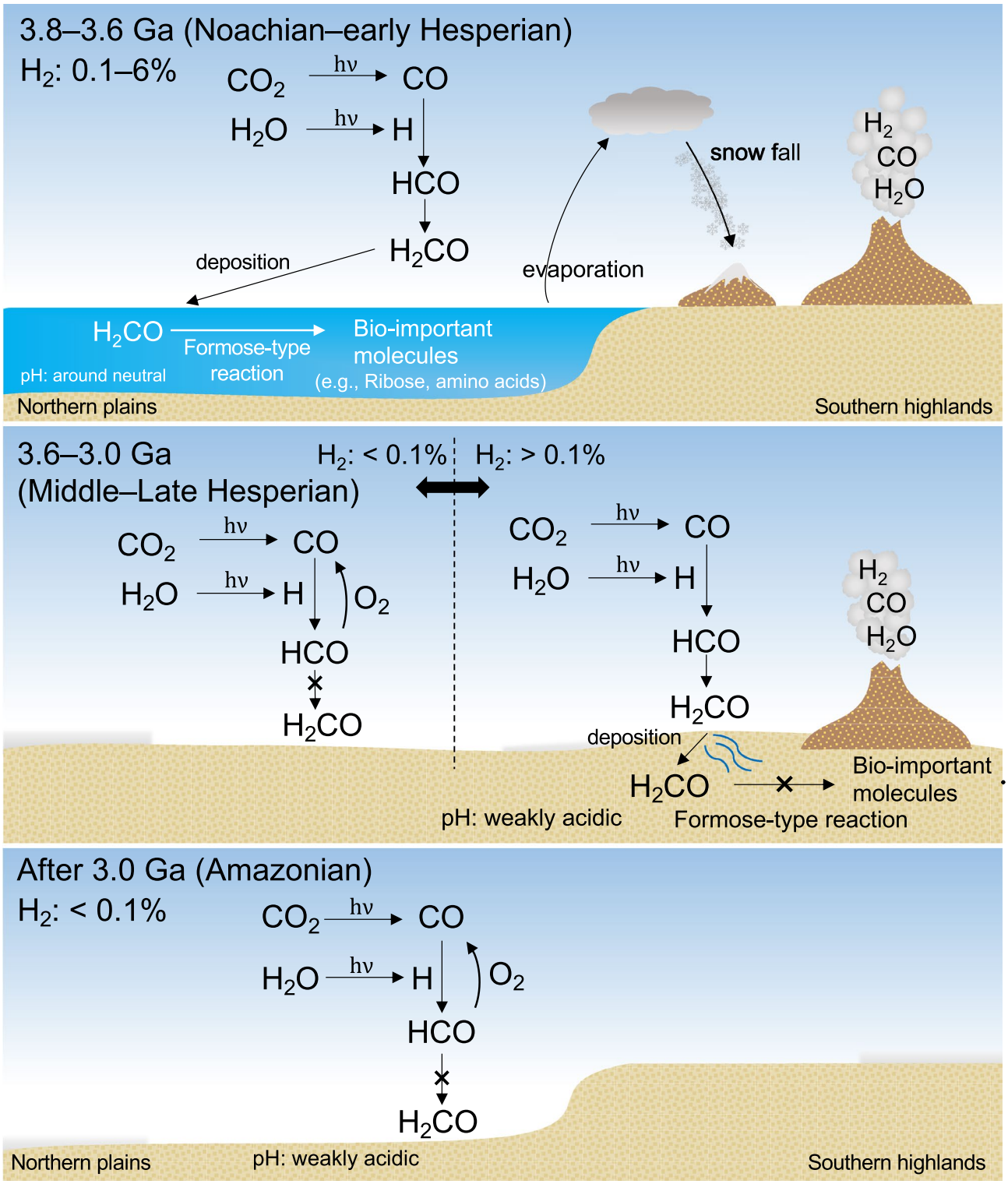

Figure 7. Scenario for the atmospheric H_2CO production at ca. 3.8–3.6 Ga (top panel), ca. 3.5–3.0 Ga (middle panel), and after ca. 3.0 Ga (bottom panel). In the Noachian and early Hesperian periods (3.8–3.6 Ga), the synthesized H_2CO in the atmosphere was deposited into the ocean, forming bio-important molecules, such as ribose. In the middle and late Hesperian (3.6–3.0 Ga), H_2CO was sporadically formed. Even in the period when H_2CO was abundantly formed, subsequent formose reaction does not proceed due to the acidic condition of the water. From the Amazonian to the present (after 3.0 Ga), the production of H_2CO is deficient, as in the case with $H_2 < 0.1\%$ in the middle and late Hesperian.

early Martian ocean, we make the following assumptions: one-third of the surface area was covered by an ocean as suggested by the analysis of the distribution of delta and valleys[47], the seawater pH at ~ 3.8 Ga in early Mars was near-neutral, as the late Noachian marked a transition period from alkaline to acidic water pH[48], early Mars had a hydrological cycle similar to Earth's ($f_R = 1$), the atmosphere contained the same fraction of glycolaldehyde as an estimated atmosphere of the early Earth[17], and the conversion rate of H_2CO into ribose was ~ 3.5×10^{-6} mol_{Rib} mol_{FA}^{-1} estimated by the formose-reaction experiment[46]. By combining the calculated H_2CO deposition flux of 3×10^9 cm^{-2} s^{-1} ($= 1 \times 10^{21}$ m^{-2} yr^{-1}), the annual ribose production in the ocean P_{rib} is estimated to be 4×10^4 kg yr^{-1} as follows:

$$P_{rib} = \frac{f_{H_2CO} S_{sea} Y_{rib} M_{rib}}{N_A}, \tag{2}$$

where f_{H_2CO} is the deposition flux of H_2CO (m^{-2} yr^{-1}), S_{sea} is the area covered by the ocean (m^2), Y_{rib} is the conversion rate of H_2CO into ribose (mol mol^{-1}), M_{rib} is the molar mass of ribose (kg mol^{-1}), and N_A is Avogadro's constant. When f_R is 0.1, the annual ribose production is estimated to be 1×10^4 kg yr^{-1}. These suggest that bio-important sugars including ribose might have been continuously formed in water bodies on the surface. In this assumption, we disregarded several H_2CO consumption processes in seawater, including photolysis, hydrolysis, and reactions with other reactive molecules such as ammonia[3,49]. It is unclear whether ammonia was present on early Mars, but it may have transiently been present in the atmosphere or in water on early Mars, potentially due to processes, such as episodic volcanic degassing or impact degassing. Previous studies on early Earth indicated that reducing gases, including ammonia, could be generated through impact events[50,51]. This process may have analogously occurred on early Mars. In the presence of ammonia, the formose reaction forms various nitrogen containing organic matter including proteinogenic amino acids[5]. Nitrogen containing organic matter has been found in a Martian meteorite[52]. The formose reaction also forms refractory organic matter, similar to cometary and meteoritic insoluble organic matter[6]. The photochemical H_2CO calculated in this study and its following formose reaction may be related to the origin of refractory and non-refractory organic matter found in the 3.5-billion-year-old lacustrine mudstones of Mars[53] and Noachian carbonates in a Martian meteorite[52]. However, it is still difficult to distinguish whether this organic matter was derived from the photochemical H_2CO. One way to distinguish them is to compare their carbon isotope compositions. The carbon isotopic analysis onboard the Curiosity rover detected an anomalously depleted ^{13}C in organic matter[54]. The deposition of photochemical H_2CO which experienced CO_2 photolysis-driven carbon isotope fractionation might explain this depletion[55]. Our future work is to include carbon isotope fractionation in the model and compare it with the isotope observation data. Significant H_2CO synthesis on the warm Noachian Mars with liquid surface water allowed for the formation of sugars and amino acids (Fig. 7). The formation of H_2CO would have sporadically continued on Hesperian to early Amazonian Mars, but the transition to an ice-covered and acidic surface environment on Hesperian Mars dramatically decreased the possibility of the formation of the building blocks of life, because the production of sugars and amino acids through the formose-type reaction substantially decreased in acidic water[46,48,56,57]. Therefore, the time period suitable for the formation of bio-important molecules on early Mars might be limited to the Noachian and potentially early Hesperian Mars, the warm climate era before the pH of the surface liquid water became acidic.

Secondary concentration processes are essential for synthesizing bio-important molecules on planetary surfaces. Early Mars may have experienced episodic warm and cold climate periods[33]. During the transition from warm to cold periods, a large amount of oceanic water would have been stored as snow on land; thus, oceanic water would have become concentrated. Such evaporative environments might further promote chemical evolution to form biopolymers, such as proteins and RNAs because the primary reaction that forms these molecules is dehydration reactions[58,59]. These reactions may have been promoted by carbonate and borate, which have been shown to be present on Mars[60–64]. Future studies considering topography and secondary concentration processes are important to elucidate the possibility of RNA synthesis on early Mars.

Conclusions

Formaldehyde (H_2CO) is a crucial organic matter in the formation of bioorganic molecules such as amino acids and ribose. We investigated the atmospheric production of H_2CO on early Mars using a one-dimensional photochemical model. We assume a 2-bar background CO_2-dominated atmosphere with various concentrations of H_2 and CO while adopting temperature and H_2O profiles from a 3-D paleo-Mars global climate model. Our results show that a larger amount of H_2 leads to a more significant production of H_2CO owing to the reduction in O_2 abundance in the lower atmosphere. Two mechanisms cause this O_2 reduction: (1) the chemical reaction with H atoms at high altitudes above 100 km, resulting in a decrease in O_2 downward flux, and (2) the HCO catalytic cycle at ~ 50–60 km reducing O_2 in the lower atmosphere below 60 km. In a warm climate, the number density of H_2CO is ~ 5×10^9 cm^{-3} near the surface, and its deposition into the ocean is 3×10^9 cm^{-2} s^{-1} assuming that early Mars had a hydrological cycle similar to Earth's. The sensitivity analysis of water vapor implies that H_2CO production could have varied locally in correlation with the abundance of water vapor. Our results suggest that a continuous supply of H_2CO could be used to form various organic compounds, including life's building blocks, such as amino acids and sugars. This photochemically produced H_2CO could be a possible origin for the organic matter observed on the Martian surface. Given the previously reported conversion rate from H_2CO to ribose, the calculated H_2CO deposition flux suggests a continuous supply of bio-important sugars on Noachian and early Hesperian Mars.

Data availability

The data of the simulation results is available at figshare repository: https://doi.org/https://doi.org/10.6084/m9.figshare.24032064.

Received: 8 September 2023; Accepted: 23 January 2024
Published online: 09 February 2024

References

1. Wordsworth, R. D. The climate of early Mars. *Annu. Rev. Earth Planet. Sci.* **44**, 381–408 (2016).
2. Carter, J., Poulet, F., Bibring, J. P. & Murchie, S. Detection of hydrated silicates in crustal outcrops in the northern plains of Mars. *Science* **328**, 1682–1686 (2010).
3. Cleaves, H. J. II. The prebiotic geochemistry of formaldehyde. *Precambrian Res.* **164**, 111–118 (2008).
4. Miller, S. L. & Urey, H. C. Organic compound synthesis on the primitive earth. *Science* **130**, 245–251 (1959).
5. Kebukawa, Y., Chan, Q. H., Tachibana, S., Kobayashi, K. & Zolensky, M. E. One-pot synthesis of amino acid precursors with insoluble organic matter in planetesimals with aqueous activity. *Sci. Adv.* **3**, e1602093 (2017).
6. Furukawa, Y., Iwasa, Y. & Chikaraishi, Y. Synthesis of ^{13}C-enriched amino acids with ^{13}C-depleted insoluble organic matter in a formose-type reaction in the early solar system. *Sci. Adv.* **7**, eabd3575 (2021).
7. Breslow, R. On the mechanism of the formose reaction. *Tetrahedron Lett.* **1**, 22–26 (1959).
8. Furukawa, Y. *et al.* Extraterrestrial ribose and other sugars in primitive meteorites. *Proc. Natl. Acad. Sci. U.S.A.* **116**, 24440–24445 (2019).
9. Gilbert, W. Origin of life: The RNA world. *Nature* **319**, 618–618 (1986).
10. Forget, F. *et al.* 3D modelling of the early martian climate under a denser CO2 atmosphere: Temperatures and CO_2 ice clouds. *Icarus* **222**, 81–99 (2013).
11. Wordsworth, R. *et al.* Global modelling of the early martian climate under a denser CO2 atmosphere: Water cycle and ice evolution. *Icarus* **222**, 1–19 (2013).
12. Ramirez, R. M. *et al.* Warming early Mars with CO2 and H2. *Nat. Geosci.* **7**, 59–63 (2014).
13. Wordsworth, R. *et al.* Transient reducing greenhouse warming on early Mars. *Geophys. Res. Lett.* **44**, 665–671 (2017).
14. Kamada, A. *et al.* A coupled atmosphere–hydrosphere global climate model of early Mars: A 'cool and wet'scenario for the formation of water channels. *Icarus* **338**, 113567 (2020).
15. Kamada, A. *et al.* Global climate and river transport simulations of early Mars around the Noachian and Hesperian boundary. *Icarus* **368**, 114618 (2021).
16. Pinto, J. P., Gladstone, G. R. & Yung, Y. L. Photochemical production of formaldehyde in Earth's primitive atmosphere. *Science* **210**, 183–185 (1980).
17. Harman, C. E., Kasting, J. F. & Wolf, E. T. Atmospheric production of glycolaldehyde under hazy prebiotic conditions. *Orig. Life Evol. Biosph.* **43**, 77–98 (2013).
18. Nakamura, Y. *et al.* Photochemical and radiation transport model for extensive use (PROTEUS). *Earth Planets Space* **75**, 140 (2023).
19. Nakamura, Y. *et al.* Effect of meteoric ions on ionospheric conductance at Jupiter. *J. Geophys. Res. Space Phys.* **127**, e2022JA030312 (2022).
20. Yoshida, T. *et al.* Strong depletion of 13C in CO induced by photolysis of CO2 in the Martian atmosphere, calculated by a photochemical model. *Planet. Sci. J.* **4**, 53 (2023).
21. Kamada, A. *et al.* Evolution of ice sheets on early Mars with subglacial river systems. *Icarus* **385**, 115117 (2022).
22. Krasnopolsky, V. A. Solar activity variations of thermospheric temperatures on Mars and a problem of CO in the lower atmosphere. *Icarus* **207**, 638–647 (2010).
23. Koyama, S. *et al.* Stability of atmospheric redox states of early Mars inferred from time response of the regulation of H and O losses. *Astrophys. J.* **912**, 135 (2021).
24. Amerstorfer, U. V. *et al.* Escape and evolution of Mars's CO2 atmosphere: Influence of suprathermal atoms. *J. Geophys. Res. Planets* **122**, 1321–1337 (2017).
25. Claire, M. W. *et al.* The evolution of solar flux from 0.1 nm to 160 μm: quantitative estimates for planetary studies. *Astrophys. J.* **757**, 95 (2012).
26. Ranjan, S. *et al.* Photochemistry of anoxic abiotic habitable planet atmospheres: impact of new H2O cross sections. *Astrophys. J.* **896**, 148 (2020).
27. Matta, M., Withers, P. & Mendillo, M. The composition of Mars' topside ionosphere: Effects of hydrogen. *J. Geophys. Res. Space Phys.* **118**, 2681–2693 (2013).
28. Hu, R., Seager, S. & Bains, W. Photochemistry in terrestrial exoplanet atmospheres. I. Photochemistry model and benchmark cases. *Astrophys. J.* **761**, 166 (2012).
29. Batalha, N., Domagal-Goldman, S. D., Ramirez, R. & Kasting, J. F. Testing the early Mars H2–CO2 greenhouse hypothesis with a 1-D photochemical model. *Icarus* **258**, 337–349 (2015).
30. Pearce, B. K. *et al.* Toward RNA life on early Earth: From atmospheric HCN to biomolecule production in warm little ponds. *Astrophys. J.* **932**, 9 (2022).
31. Giorgi, F. & Chameides, W. L. The rainout parameterization in a photochemical model. *J. Geophys. Res. Atmos.* **90**, 7872–7880 (1985).
32. Haberle, R. M., Zahnle, K., Barlow, N. G. & Steakley, K. E. Impact degassing of H2 on early Mars and its effect on the climate system. *Geophys. Res. Lett.* **46**, 13355–13362 (2019).
33. Wordsworth, R. *et al.* A coupled model of episodic warming, oxidation and geochemical transitions on early Mars. *Nat. Geosci.* **14**, 127–132 (2021).
34. Pan, L. & Deng, Z. Bizzarro M (2023) Impact induced oxidation and its implications for early Mars climate. *Geophys. Res. Lett.* **50**, e2023GL102724 (2023).
35. Chassefière, E., Lasue, J., Langlais, B. & Quesnel, Y. Early Mars serpentinization-derived CH4 reservoirs, H2-induced warming and paleopressure evolution. *Meteorit. Planet. Sci.* **51**, 2234–2245 (2016).
36. Zahnle, K., Haberle, R. M., Catling, D. C. & Kasting, J. F. Photochemical instability of the ancient Martian atmosphere. *J. Geophys. Res. Planets* **113**, E11 (2008).
37. Kasting, J. F. Bolide impacts and the oxidation state of carbon in the Earth's early atmosphere. *Orig. Life Evol. Biosph.* **20**, 199–231 (1990).
38. Kharecha, P., Kasting, J. & Siefert, J. A coupled atmosphere–ecosystem model of the early Archean Earth. *Geobiology* **3**, 53–76 (2005).
39. Reilly, J. P., Clark, J. H., Moore, C. B. & Pimentel, G. C. HCO production, vibrational relaxation, chemical kinetics, and spectroscopy following laser photolysis of formaldehyde. *J. Chem. Phys.* **69**, 4381–4394 (1978).
40. McElroy, M. B. & Donahue, T. M. Stability of the Martian atmosphere. *Science* **177**, 986–988 (1972).
41. Ramirez, R. M. *et al.* Warming early Mars with CO2 and H2. *Nat. Geosci.* **7**, 59–63 (2014).

42. Grott, M., Morschhauser, A., Breuer, D. & Hauber, E. Volcanic outgassing of CO2 and H2O on Mars. *Earth Planet. Sci. Lett.* **308**, 391–400 (2011).
43. Cartier, C. *et al.* Experimental study of trace element partitioning between enstatite and melt in enstatite chondrites at low oxygen fugacities and 5 GPa. *Geochim. Cosmochim. Acta* **130**, 167–187 (2014).
44. Masuda, S., Furukawa, Y. & Kobayashi, T. Experimental investigation of the formation of formaldehyde by Hadean and Noachian impacts. *Astrobiology* **21**, 413–420 (2021).
45. Korablev, O. I. *et al.* Tentative identification of formaldehyde in the Martian atmosphere. *Planet. Space sci.* **41**, 441–451 (1993).
46. Ono, C., et al. Abiotic ribose synthesis under aqueous environments with various chemical conditions. Submitted to Astrobiology.
47. Di, A. G. & Hynek, B. M. Ancient Ocean on Mars supported by global distribution of deltas and valleys. *Nat. Geosci* **3**, 459–463 (2010).
48. Hurowitz, J. A., Fischer, W. W., Tosca, N. J. & Milliken, R. E. Origin of acidic surface waters and the evolution of atmospheric chemistry on early Mars. *Nat. Geosci.* **3**, 323–326 (2010).
49. Zhang, Z. *et al.* Evaluating the abiotic synthesis potential and the stability of building blocks of life beneath an impact-induced steam atmosphere. *Front. Microbiol.* **14**, 1032073 (2023).
50. Hashimoto, G. L., Abe, Y. & Sugita, S. The chemical composition of the early terrestrial atmosphere: Formation of a reducing atmosphere from CI-like material. *J. Geophys. Res. Planets* **112**, E5 (2007).
51. Shimamura, K., Shimojo, F., Nakano, A. & Tanaka, S. Meteorite impact-induced rapid NH_3 production on early Earth: Ab Initio molecular dynamics simulation. *Sci. Rep.* **6**, 38953 (2016).
52. Koike, M. *et al.* In-situ preservation of nitrogen-bearing organics in Noachian Martian carbonates. *Nat. Commun.* **11**, 1988 (2020).
53. Stern, J. C., Malespin, C. A. & Eigenbrode, J. L. Organic carbon concentrations in 3.5-billion-year-old lacustrine mudstones of Mars. *Proc. Natl. Acad. Sci. USA* **119**, e2201139119 (2022).
54. House, C. H. *et al.* Depleted carbon isotope compositions observed at Gale crater. *Mars. Proc. Natl. Acad. Sci. USA* **119**, e2115651119 (2022).
55. Ueno, Y. et al. Anomalously 13C-depleted organic matter from CO in early Mars atmosphere, 19 December 2022, PREPRINT (Version 1) available at Research Square https://doi.org/10.21203/rs.3.rs-2312052/v1
56. Bibring, J. P. *et al.* Global mineralogical and aqueous Mars history derived from OMEGA/Mars express data. *Science* **312**, 400–404 (2006).
57. Ehlmann, B. L. *et al.* Clay minerals in delta deposits and organic preservation potential on Mars. *Nat. Geosci.* **1**, 355–358 (2008).
58. Lohrmann, R. & Orgel, L. E. Urea-inorganic phosphate mixtures as prebiotic phosphorylating agents. *Science* **171**, 1–5 (1968).
59. Rodriguez-Garcia, M. *et al.* Formation of oligopeptides in high yield under simple programmable conditions. *Nat. Commun.* **6**, 8385 (2015).
60. Becker, S. *et al.* Unified prebiotically plausible synthesis of pyrimidine and purine RNA ribonucleotides. *Science* **366**, 76–82 (2019).
61. Toner, J. D. & Catling, D. C. A carbonate-rich lake solution to the phosphate problem of the origin of life. *Proc. Natl. Acad. Sci. USA* **117**, 883–888 (2020).
62. Gasda, *et al.* In situ detection of boron by ChemCam on Mars. *Geophys. Res. Lett.* **44**, 8739–8748 (2017).
63. Ricardo, A., Carrigan, M. A., Olcott, A. N. & Benner, S. A. Borate minerals stabilize ribose. *Science* **303**, 196 (2004).
64. Sumie, Y. *et al.* Boron-assisted abiotic polypeptide synthesis. *Commun. Chem.* **6**, 89 (2023).

Acknowledgements

This work was supported by the International Joint Graduate Program in Earth and Environmental Sciences, Tohoku University (GP-EES). S.K. was supported by JSPS KAKENHI Grant Number JP22KJ0314. A.K. was supported by JSPS KAKENHI Grant Number JP23K13166. N.T. was supported by JSPS KAKENHI Grant Numbers JP19H00707, JP20H00192, and JP22H00164. Y.N. was supported by JSPS KAKENHI Grant Number JP22KJ0280. N.T. and Y.F. were supported by NINS Astrobiology Center satellite research.

Author contributions

S.K., Y.F., and N.T. designed the study. S.K. performed the photochemical calculation. S.K., Y.N., and T.Y. developed the photochemical model. A.K. and T.K. developed the GCM model, and A.K. performed its calculation. S.K. took the lead in writing the manuscript. All authors interpreted the results and improved the manuscript.

Competing interests

The authors declare no competing interests.

Additional information

Supplementary Information The online version contains supplementary material available at https://doi.org/10.1038/s41598-024-52718-9.

Correspondence and requests for materials should be addressed to S.K.